Cardiovasc Intervent Radiol (2019) 42:1771–1776
https://doi.org/10.1007/s00270-019-02336-0

CT Texture Analysis and Machine Learning Improve Post-ablation Prognostication in Patients with Adrenal Metastases: A Proof of Concept

Dania Daye[1] · Pedro V. Staziaki[2] · Vanessa Fiorini Furtado[3] · Azadeh Tabari[1] · Florian J. Fintelmann[1] · Nathan Elie Frenk[1] · Paul Shyn[4] · Kemal Tuncali[4] · Stuart Silverman[4] · Ronald Arellano[1] · Michael S. Gee[1] · Raul Nirmal Uppot[1]

Received: 23 May 2019 / Accepted: 30 August 2019 / Published online: 5 September 2019

Abstract

Introduction To assess the performance of pre-ablation computed tomography texture features of adrenal metastases to predict post-treatment local progression and survival in patients who underwent ablation using machine learning as a prediction tool.

Materials and Methods This is a pilot retrospective study of patients with adrenal metastases undergoing ablation. Clinical variables were collected. Thirty-two texture features were extracted from manually segmented adrenal tumors. A univariate cox proportional hazard model was used for prediction of local progression and survival. A linear support vector machine (SVM) learning technique was applied to the texture features and clinical variables, with leave-one-out cross-validation. Receiver operating characteristic analysis and the area under the curve (AUC) were used to assess performance between using clinical variables only versus clinical variables and texture features.

Results Twenty-one patients (61% male, age 64.1 ± 10.3 years) were included. Mean time to local progression was 29.8 months. Five texture features exhibited association with progression ($p < 0.05$). The SVM model based on clinical variables alone resulted in an AUC of 0.52, whereas the SVM model that included texture features resulted in an AUC 0.93 ($p = 0.01$). Mean overall survival was 35 months. Fourteen texture features were associated with survival in the univariate model ($p < 0.05$). While the trained SVM model based on clinical variables resulted in an AUC of 0.68, the SVM model that included texture features resulted in an AUC of 0.93 ($p = 0.024$).

Discussion Pre-ablation texture analysis and machine learning improve local tumor progression and survival prediction in patients with adrenal metastases who undergo ablation.

Keywords Radiomics · Machine learning · Prognostication · Texture analysis · Ablation · Adrenal metastasis

Dania Daye and Pedro V. Staziaki contributed equally to this work.

Electronic supplementary material The online version of this article (https://doi.org/10.1007/s00270-019-02336-0) contains supplementary material, which is available to authorized users.

✉ Dania Daye
ddaye@mgh.harvard.edu

[1] Department of Radiology, Massachusetts General Hospital, Harvard Medical School, 55 Fruit Street, GRB #290, Boston, MA 02114, USA

[2] Department of Radiology, Boston Medical Center, Boston University School of Medicine, Boston, MA, USA

[3] Department of Internal Medicine, University of Massachusetts, UMass, Worcester, MA, USA

[4] Department of Radiology, Brigham and Women's Hospital, Harvard Medical School, Boston, MA, USA

Introduction

Adrenal metastases can occur in 3–27% of patients with malignancy, according to autopsy series [1, 2]. Percutaneous ablation is an important minimally invasive treatment option for patients with metastatic cancer with comorbidities and has been found to be safe [3]. Reported

local recurrence-free survival rates range from 75 to 88% at 1 year [4–14], but data on predictors of post-ablation progression and survival are limited.

Computed tomography (CT) texture analysis has been reported to predict treatment outcome in patients with non-small cell lung cancer, hepatocellular carcinoma, colorectal cancer and metastatic renal cell carcinoma (RCC) [15–17]. Image texture on CT is defined as the pattern of variation in voxel intensity levels in an image. Texture analysis allows the mathematic detection of the spatial arrangement of gray levels among adjacent pixels [18, 19]. By extracting information native to image data, most of which are not perceived by the human eye, texture analysis is part of a larger selection of image analysis data points that comprise what we call "radiomics."

Machine learning is a branch of artificial intelligence that can be used to extract meaningful patterns from a large number of variables or observations by identifying the best combination of data. Because this technology analyzes patterns that are beyond human visual perception, it has the potential to unveil predictive models unachievable by standard radiologist interpretation [20]. When applied to medical imaging, machine learning is a powerful tool for diagnosis [21], with myriad potential clinical applications, including polyp detection with virtual colonoscopy [22], breast cancer diagnosis on mammography [23] and body composition analysis on abdominal CT [24].

The objective of this study was to assess the role of pre-ablation CT texture analysis and support vector machine learning in improving outcome prediction following ablation of adrenal metastases. The outcomes of interest were post-ablation local tumor progression and survival.

Materials and Methods

Study Design

This retrospective study was approved by the IRB, which waive the need for consent. All patients who had biopsy-proven adrenal metastases treated with image-guided percutaneous thermal ablation at two large academic medical centers between July 2002 and June 2016 were included. Exclusion criteria were (1) tumor size $\geq$ 5 cm, (2) procedures performed for local debulking and/or symptomatic relief without curative intent, (3) patients who did not have an abdominal CT with intravenous contrast within 3 months prior to ablation and (4) patients without follow-up within 6 months after ablation at our institution.

Clinical variables collected from the electronic medical record were age, sex assigned at birth, tumor size, ablation modality, tumor sidedness, administration of chemotherapy, tumor histology and technical success. Technical success was defined as imaging confirmation of complete tumor ablation with no visible residual tumor either after the first ablation or after a second ablation completed within 4 months of the first ablation.

The two outcomes of interest in this study were the presence of post-ablation local progression and death. Local tumor progression was defined as the development of new enhancing tumor during follow-up after documentation of technical success. Follow-up ended with the most recent clinic visit or most recent imaging study before September 2016 or with the patient's death.

Imaging Acquisition

All patients included in this study underwent contrast-enhanced CT studies performed either on a 16-slice LightSpeed (GE Health care, Milwaukee, Wisconsin) or a 40-slice SOMATOM Sensation Open (Siemens Medical Solutions, Forchheim, Germany) scanner. The scans were obtained in the portal venous phase 70 s after administration of IV contrast material. A total of 80–120 mL of nonionic iodinated contrast material (370 mg I/mL) was injected IV at 3 mL/s in all patients. The scanning protocols and parameters included reconstruction with slice thickness of 5 mm, weight-based tube potential of 100–140 kV (88 scans at 120 kV, 10 scans at 140 kV and three scans at 100 kV), automatic tube current modulation (75–500 mAs) and 0.5-s gantry rotation time. These CT images were retrieved from the picture archiving and communication system (Agfa PACS; Amsterdam, Netherlands).

Image Segmentation and Texture Analysis

All lesions were manually contoured by a single radiologist who was blinded to patient history. All segmentation was performed on axial images using soft tissue window settings based on the image containing the large cross-sectional area of the lesion. A single region of interest (ROI) was created for each lesion.

Following manual segmentation, a MATLAB (MathWorks, Natick, Massachusetts) texture analysis software extracted 32 texture features from each segmented volume. The mean value of the textural features on a region of interest (ROI) basis was estimated. The volume of each primary tumor was also calculated. The 32 features included 14 gray-level co-occurrence matrix (GLCM or Haralick) features, 15 Laws features and 3 Tamura features [18, 25–28].

Statistical Analysis and Machine Learning

Tumor characteristics, available for all participants, are presented as frequency (percentage) for categorical data and mean ± standard deviation for continuous data.

A univariate cox proportional hazards regression model was used to assess the hazard ratios of texture features associated with tumor progression or mortality. The proportional hazards assumption was met in all models, and all models fit the data. All hazard ratios below 0.01 were rounded to < 0.01 and above 100 to > 100. Event curves were determined according to the Kaplan–Meier method, and comparisons of cumulative event rates were performed by the log-rank test.

A linear support vector machine (SVM) learning model was used to predict each of the two outcomes of interest. Leave-one-out cross-validation was used, running the model 21 times, every time taking one patient out (Fig. 1). After that, an SVM model that included only clinical data and an SVM model that included both texture features and clinical data to predict each of the two outcomes of interest were created. Receiver operating characteristic (ROC) analysis and the area under the curve (AUC) were used to assess classification performance. Both models' ROC curves were compared using the DeLong Test [29].

All statistical analyses and machine learning models were performed using Stata (Stata Statistical Software: Release 14. StataCorp. 2015. College Station, TX: StataCorp LP). A two-sided p value of < 0.05 was considered statistically significant.

Results

Patient Characteristics

From July 2002 and June 2016, 60 patients underwent thermal ablation of adrenal metastases. Of these patients, 16 (27%) were excluded because of tumor size > 5 cm, 4 (7%) were excluded because ablation was performed for palliation, and 19 (32%) were lost to follow-up. This resulted in 21 patients with 21 adrenal tumors that were treated with 21 procedures. This series included patients from a previously published investigation [14]. The mean follow-up period was 35 ± 29 months. Mean tumor diameter was 3.0 ± 0.8 cm. Additional details of the cohort are presented in Table 1.

Predictors of Local Progression

Mean time to local progression was 29.8 ± 29.7 months. Only the 5 Haralick image features were associated with local progression in the univariate model (Electronic Supplementary Material Table 2). The SVM model based on

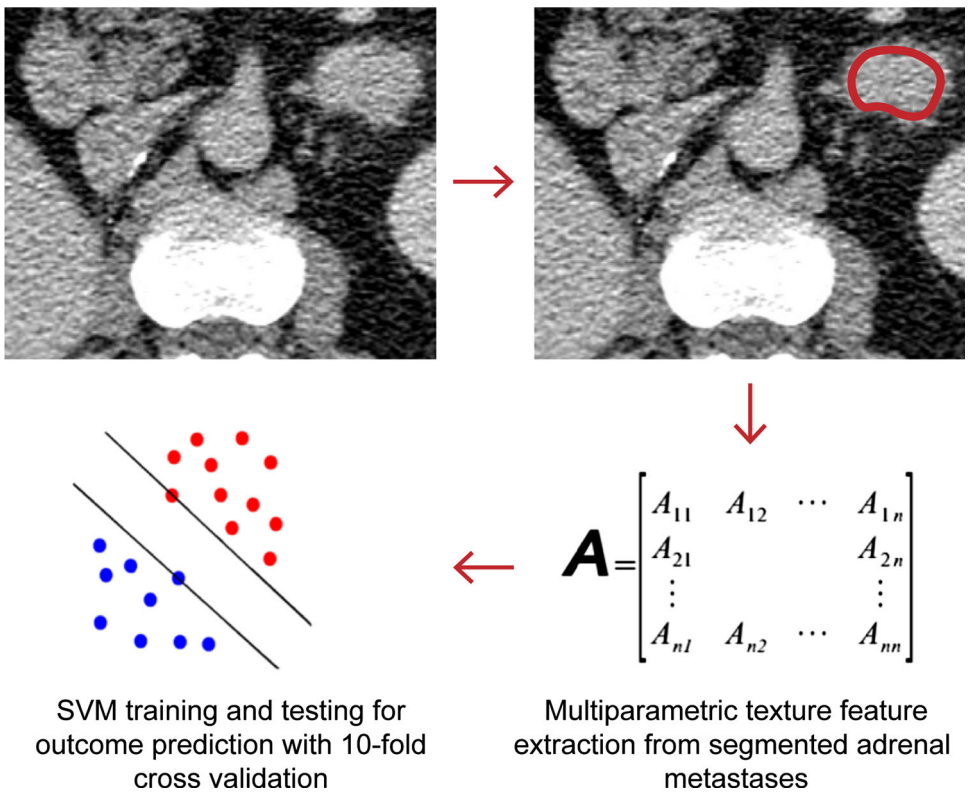

Fig. 1 Image segmentation and machine learning

Table 1 Patient characteristics

Patient demographics	$n = 21$
Age	64.1 ± 10.3
Male sex	13 (61%)
Tumor size (cm)	3.0 ± 0.8
Ablation modality	
Cryoablation	11 (53%)
Radiofrequency	7 (33%)
Microwave	3 (14%)
Right tumor side	12 (57%)
Post-ablation chemotherapy	19 (76%)
Primary tumor	
RCC	7 (33%)
NSCLC	4 (19%)
Other	10 (48%)
Exclusively adrenal disease	16 (76%)
Technical success	20 (95%)

the clinical variables utilized (age, sex assigned at birth, tumor size, ablation modality, tumor sidedness, administration of chemotherapy, tumor histology and technical success) demonstrated an accuracy of 0.52, whereas the SVM including texture features in addition to clinical variables resulted in an accuracy of 0.93 (Fig. 2). The two accuracies were statistically different ($p = 0.001$).

Predictors of Survival

Mean patient survival was 35 ± 30 months. In the univariate model, 14 image features were associated with patient survival (7 Law and 7 Haralick features, Electronic Supplementary Material Table 3). The SVM model based on the clinical parameters resulted in an AUC of 0.68. An SVM model that includes texture analysis features in addition to clinical variables resulted in performance of 0.93 (Fig. 3). The two models were statistically different ($p = 0.024$).

Discussion

Adrenal metastases can have a wide range of features on CT, including an irregular shape and heterogeneous attenuation. Texture analysis can capture tumor characteristics not currently represented by clinical prognostic markers by extracting quantitative high-dimensional data from digital medical images. This process is part of radiomics and might become one of the many computer-based tools to improve our diagnostic capabilities in the future [30].

Texture analysis of CT and magnetic resonance (MR) images has been used to diagnose adrenal lesion, both with and without machine learning. For instance, one study has shown that it is possible to differentiate between benign and metastatic adrenal masses in patients with RCC based on CT imaging features, including attenuation and texture information [31]. However, another study found that it was not possible to reliably differentiate adenomas from metastases using subjective descriptive characteristics (smooth margin, rim enhancement, central vein sign and homogeneity) as well as texture analysis in a single-phase contrast-enhanced CT [32]. On MR, it is possible to differentiate clear cell RCC metastases to the adrenal gland from adenomas using subjective and quantitative analyses such as T2-weighted signal intensity and heterogeneity [33]. Another study using machine learning-based quantitative texture analysis on unenhanced CT found that they were a reliable quantitative method in differentiating pheochromocytoma from lipid-poor adenoma [34].

Given the large amount of data that can be derived from medical images, machine learning methods are useful to make sense of the data and help predict outcomes. Machine learning was used in this study instead of a multivariate

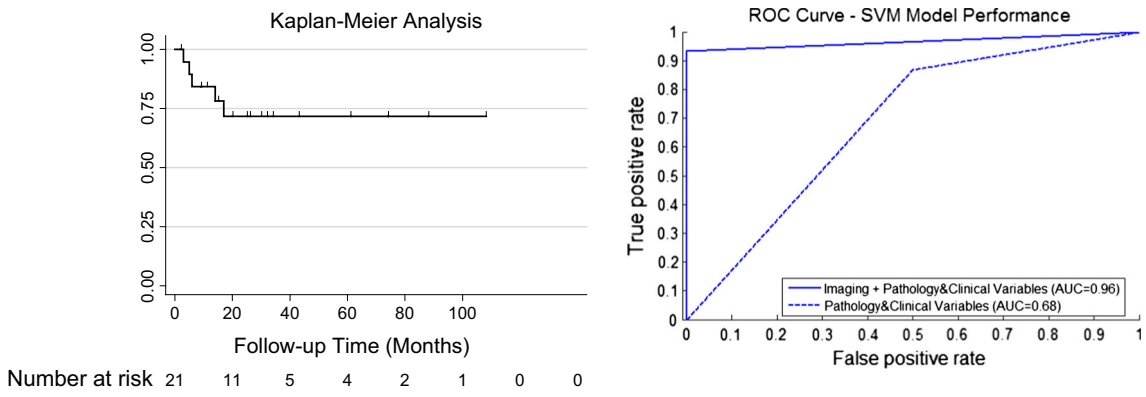

Fig. 2 Kaplan–Meier curve and receiver operating characteristic curve for tumor progression

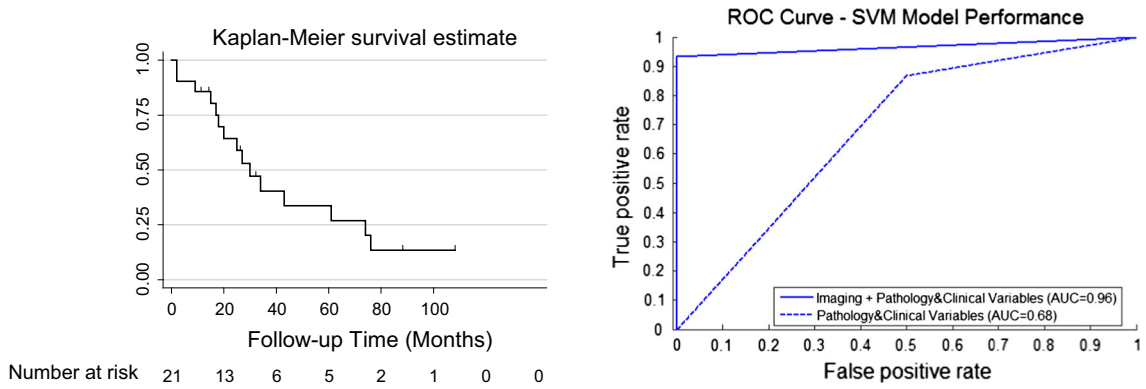

Fig. 3 Kaplan–Meier curve and receiver operating characteristic curve for overall survival

logistic regression because the former can deal with a larger number of features, is more robust and is resistant to overfitting. In addition, we used machine learning to assess the accuracy of two different groups of predictors, that is, clinical variables alone versus texture analysis features in addition to clinical variables.

This study showed that the addition of texture features derived from routine pre-procedural CT images significantly improved the accuracy of models predicting local progression and overall survival following thermal ablation of adrenal metastases. Our study extends beyond the previous literature to use CT texture analysis as a tool to predict patient outcomes following adrenal metastasis ablation. In this case, the histologic diagnosis is already established and the CT texture features are being used as a marker of biological aggressiveness and responsiveness to percutaneous ablation.

CT-guided ablation can achieve local control for adrenal metastases measuring less than 5 cm with previous studies showing overall survival rates at 1, 3 and 5 years of 82%, 44% and 34%, respectively [14]. Another study found that 1- , 3- and 5-year overall survival rates of patients who received radiofrequency ablation were 75%, 34% and 30%, with a median survival time of 26 months [6]. Our results show the added benefit of CT texture features in predicting local recurrence and survival in this population. Knowing which patients are at higher risk of local recurrence following adrenal ablation would be useful in guiding both ablation planning (e.g., wider ablation margins) and post-imaging imaging algorithms (e.g., more frequent imaging).

This study has to be interpreted within its limitations. First, this was a proof-of-concept pilot retrospective study with a small cohort. Additional studies with more patients are necessary to validate texture analysis for this application. Moreover, the CT protocols including the types of CT scanners may not have been identical between subjects and between the two hospitals where the CT images were acquired, which may potentially affect the texture analysis. The question whether texture analysis translates to other practice settings with different image acquisition protocols remains to be answered.

Conclusion

Machine learning-based predictive models incorporating pre-ablation texture analysis may improve prognostication following thermal ablation of adrenal metastases. Machine learning predicted both local recurrence and survival in this small cohort and showed a remarkable increase in accuracy to more than 95% when CT-derived texture features were included.

Funding This study was not supported by any funding.

Compliance with Ethical Standards

Conflict of interest The authors declare that they have no conflict of interest.

Ethical Approval All procedures performed in studies involving human participants were in accordance with the ethical standards of the institutional and/or national research committee and with the 1964 Helsinki Declaration and its later amendments or comparable ethical standards.

References

1. Abrams HL, Spiro R, Goldstein N. Metastases in carcinoma; analysis of 1000 autopsied cases. Cancer. 1950;3(1):74–85.
2. Lam KY, Lo CY. Metastatic tumours of the adrenal glands: a 30-year experience in a teaching hospital. Clin Endocrinol. 2002;56(1):95–101.
3. Fintelmann FJ, Tuncali K, Puchner S, Gervais DA, Thabet A, Shyn PB, et al. Catecholamine surge during image-guided ablation of adrenal gland metastases: predictors, consequences, and recommendations for management. J Vasc Interv Radiol. 2016;27(3):395–402. https://doi.org/10.1016/j.jvir.2015.11.034.

4. Wang Y, Liang P, Yu X, Cheng Z, Yu J, Dong J. Ultrasound-guided percutaneous microwave ablation of adrenal metastasis: preliminary results. Int J Hyperthermia. 2009;25(6):455–61. https://doi.org/10.1080/02656730903066608.
5. Li X, Fan W, Zhang L, Zhao M, Huang Z, Li W, et al. CT-guided percutaneous microwave ablation of adrenal malignant carcinoma: preliminary results. Cancer. 2011;117(22):5182–8. https://doi.org/10.1002/cncr.26128.
6. Hasegawa T, Yamakado K, Nakatsuka A, Uraki J, Yamanaka T, Fujimori M, et al. Unresectable adrenal metastases: clinical outcomes of radiofrequency ablation. Radiology. 2015;277(2):584–93. https://doi.org/10.1148/radiol.2015142029.
7. Kuehl H, Stattaus J, Forsting M, Antoch G. Transhepatic CT-guided radiofrequency ablation of adrenal metastases from hepatocellular carcinoma. Cardiovasc Interv Radiol. 2008;31(6):1210–4. https://doi.org/10.1007/s00270-008-9377-6.
8. Mouracade P, Dettloff H, Schneider M, Debras B, Jung JL. Radio-frequency ablation of solitary adrenal gland metastasis from renal cell carcinoma. Urology. 2009;74(6):1341–3. https://doi.org/10.1016/j.urology.2009.06.058.
9. Welch BT, Callstrom MR, Carpenter PC, Wass CT, Welch TL, Boorjian SA, et al. A single-institution experience in image-guided thermal ablation of adrenal gland metastases. J Vasc Interv Radiol. 2014;25(4):593–8. https://doi.org/10.1016/j.jvir.2013.12.013.
10. Yamakado K, Anai H, Takaki H, Sakaguchi H, Tanaka T, Kichikawa K, et al. Adrenal metastasis from hepatocellular carcinoma: radiofrequency ablation combined with adrenal arterial chemoembolization in six patients. AJR Am J Roentgenol. 2009;192(6):W300–5. https://doi.org/10.2214/ajr.08.1752.
11. Wolf FJ, Dupuy DE, Machan JT, Mayo-Smith WW. Adrenal neoplasms: effectiveness and safety of CT-guided ablation of 23 tumors in 22 patients. Eur J Radiol. 2012;81(8):1717–23. https://doi.org/10.1016/j.ejrad.2011.04.054.
12. Carrafiello G, Lagana D, Recaldini C, Giorgianni A, Ianniello A, Lumia D, et al. Imaging-guided percutaneous radiofrequency ablation of adrenal metastases: preliminary results at a single institution with a single device. Cardiovasc Interv Radiol. 2008;31(4):762–7. https://doi.org/10.1007/s00270-008-9337-1.
13. Ren C, Liang P, Yu XL, Cheng ZG, Han ZY, Yu J. Percutaneous microwave ablation of adrenal tumours under ultrasound guidance in 33 patients with 35 tumours: a single-centre experience. Int J Hyperthermia. 2016;32(5):517–23. https://doi.org/10.3109/02656736.2016.1164905.
14. Frenk NE, Daye D, Tuncali K, Arellano RS, Shyn PB, Silverman SG, et al. Local control and survival after image-guided percutaneous ablation of adrenal metastases. J Vasc Interv Radiol. 2018;29(2):276–84. https://doi.org/10.1016/j.jvir.2017.07.026.
15. Goh V, Ganeshan B, Nathan P, Juttla JK, Vinayan A, Miles KA. Assessment of response to tyrosine kinase inhibitors in metastatic renal cell cancer: CT texture as a predictive biomarker. Radiology. 2011;261(1):165–71. https://doi.org/10.1148/radiol.11110264.
16. Miles KA, Ganeshan B, Griffiths MR, Young RC, Chatwin CR. Colorectal cancer: texture analysis of portal phase hepatic CT images as a potential marker of survival. Radiology. 2009;250(2):444–52. https://doi.org/10.1148/radiol.2502071879.
17. Ganeshan B, Goh V, Mandeville HC, Ng QS, Hoskin PJ, Miles KA. Non-small cell lung cancer: histopathologic correlates for texture parameters at CT. Radiology. 2013;266(1):326–36. https://doi.org/10.1148/radiol.12112428.
18. Tang X. Texture information in run-length matrices. IEEE Trans Image Process. 1998;7(11):1602–9. https://doi.org/10.1109/83.725367.
19. Haralick RM, Shanmugam K, Dinstein I. Textural features for image classification. IEEE Trans Syst Man Cybern. 1973;3(6):610–21. https://doi.org/10.1109/tsmc.1973.4309314.
20. Mayo RC, Leung J. Artificial intelligence and deep learning—radiology's next frontier? Clin Imaging. 2018;49:87–8. https://doi.org/10.1016/j.clinimag.2017.11.007.
21. Erickson BJ, Korfiatis P, Akkus Z, Kline TL. Machine learning for medical imaging. Radiographics. 2017;37(2):505–15. https://doi.org/10.1148/rg.2017160130.
22. Yoshida H, Nappi J. CAD in CT colonography without and with oral contrast agents: progress and challenges. Comput Med Imaging Graph. 2007;31(4–5):267–84. https://doi.org/10.1016/j.compmedimag.2007.02.011.
23. Chan HP, Lo SC, Sahiner B, Lam KL, Helvie MA. Computer-aided detection of mammographic microcalcifications: pattern recognition with an artificial neural network. Med Phys. 1995;22(10):1555–67. https://doi.org/10.1118/1.597428.
24. Lee H, Troschel FM, Tajmir S, Fuchs G, Mario J, Fintelmann FJ, et al. Pixel-level deep segmentation: artificial intelligence quantifies muscle on computed tomography for body morphometric analysis. J Digit Imaging. 2017;30(4):487–98. https://doi.org/10.1007/s10278-017-9988-z.
25. Castellano G, Bonilha L, Li LM, Cendes F. Texture analysis of medical images. Clin Radiol. 2004;59(12):1061–9. https://doi.org/10.1016/j.crad.2004.07.008.
26. Haralick RM, Shanmugam K. Textural features for image classification. IEEE Trans Syst Man Cybern. 1973;6:610–21.
27. Hau CC. Handbook of pattern recognition and computer vision. Singapore: World Scientific; 2015.
28. Laws KI. Textured image segmentation: University of Southern California Los Angeles Image Processing INST; 1980.
29. DeLong ER, DeLong DM, Clarke-Pearson DL. Comparing the areas under two or more correlated receiver operating characteristic curves: a nonparametric approach. Biometrics. 1988;44(3):837–45.
30. Gillies RJ, Kinahan PE, Hricak H. Radiomics: images are more than pictures, they are data. Radiology. 2016;278(2):563–77. https://doi.org/10.1148/radiol.2015151169.
31. Sasaguri K, Takahashi N, Takeuchi M, Carter RE, Leibovich BC, Kawashima A. Differentiation of benign from metastatic adrenal masses in patients with renal cell carcinoma on contrast-enhanced CT. AJR Am J Roentgenol. 2016;207(5):1031–8. https://doi.org/10.2214/ajr.16.16193.
32. Tu W, Verma R, Krishna S, McInnes MDF, Flood TA, Schieda N. Can adrenal adenomas be differentiated from adrenal metastases at single-phase contrast-enhanced CT? AJR Am J Roentgenol. 2018;211(5):1044–50. https://doi.org/10.2214/ajr.17.19276.
33. Schieda N, Krishna S, McInnes MDF, Moosavi B, Alrashed A, Moreland R, et al. Utility of MRI to differentiate clear cell renal cell carcinoma adrenal metastases from adrenal adenomas. AJR Am J Roentgenol. 2017;209(3):W152–9. https://doi.org/10.2214/ajr.16.17649.
34. Yi X, Guan X, Chen C, Zhang Y, Zhang Z, Li M, et al. Adrenal incidentaloma: machine learning-based quantitative texture analysis of unenhanced CT can effectively differentiate sPHEO from lipid-poor adrenal adenoma. J Cancer. 2018;9(19):3577–82. https://doi.org/10.7150/jca.26356.